Article

Influence of Ag Doping on Wide-Emperature Tribological Properties of γ-Fe$_2$O$_3$@SiO$_2$ Nanocomposite Coatings on Steel

Qunfeng Zeng [1,*] **, Shichuan Sun** [1] **and Qian Jia** [2]

1   Key Laboratory of Education Ministry for Modern Design and Rotor-Bearing System, Xi'an Jiaotong University, Xi'an 710049, China; sunsc719@163.com
2   School of Mechanical Engineering, City College, Xi'an Jiaotong University, Xi'an 710018, China; qianjia@mail.xjtu.edu.cn
*   Correspondence: zengqf1949@gmail.com

Abstract: γ-Fe$_2$O$_3$@SiO$_2$-Ag nanocomposite coatings were prepared to investigate the lubrication performances of the nanocomposite coatings under a wide range of temperatures. The effect of Ag doping on the tribological properties of γ-Fe$_2$O$_3$@SiO$_2$-Ag nanocomposite coatings was studied from room temperature to 600 °C, and the synergistic effect of Ag and oxides in the nanocomposite coatings was investigated. The coefficient of friction and the wear rate of γ-Fe$_2$O$_3$@SiO$_2$-Ag nanocomposite coatings decrease with an increase in Ag content. The tribological properties of 24 wt.%Ag of the nanocomposite coatings are excellent. The stable coefficient of friction is 0.25 at 100 °C and the coefficient of friction is reduced to 0.05 at 500 °C. It was found that the synergistic effect of γ-Fe$_2$O$_3$ and Ag is helpful in improving the tribological properties of γ-Fe$_2$O$_3$@SiO$_2$-Ag nanocomposite coatings over a wide temperature range. Ag plays a lubricating role at low and medium temperatures and oxides play a role in lubrication at high temperatures.

Keywords: γ-Fe$_2$O$_3$@SiO$_2$-Ag nanocomposite coatings; low friction; wide temperature range

1. Introduction

Nanocomposite coatings have been widely used as protective coatings at high temperatures owing to their superior mechanical properties over a broad range of operating temperatures [1–3]. Achieving and maintaining low friction and high wear resistances at high temperatures are some of the most challenging problems in the field of tribology, especially in the development of new-generation gas turbine engines, advanced jet engines, and powder-generating systems operating at high temperatures [4–7]. However, there is still space for improvement regarding the tribological properties of the nanocomposite coatings. Varied temperature service conditions are the typical operating environment, especially in aerospace. One of the current challenges for modern industrial tribological systems is to solve the wear and lubrication problem under varied temperature conditions. Therefore, the tribological properties of the nanocomposite coatings should be improved under a wide range of temperatures. Oxides, as high-temperature solid lubricants, cannot exhibit low friction and high wear resistance at low temperatures [8–10]. Soft noble metals, such as silver, may provide effective lubrications below 500 °C [11–16]. High-performance and low-cost Fe$_2$O$_3$-based nanocomposites are intensively investigated for their potential applications at elevated temperatures. In a previous study about the tribological properties of γ-Fe$_2$O$_3$@SiO$_2$ nanocomposite coatings, it was found that the CoF (coefficient of friction) of γ-Fe$_2$O$_3$@SiO$_2$ nanocomposite coatings is high at low temperatures and that the CoF curve fluctuates [11,17,18]. Many researchers have shown that doping improves the mechanical and tribological properties of nanocomposites [19,20]. Silver is one of the most commonly used doping elements in nanocomposite coatings [21]. Thus far, many researchers have shown that soft noble Ag metals possess stable thermochemistry behavior in mid–low temperatures, and they also have lubricating properties under moderate

temperature conditions [22,23]. The research shows that Ag doping was found to cause significant changes in the properties of coatings. The hardness and Young's modulus of coatings decreased from 22 GPa to 26 GPa to 15–17 GPa and from 260 GPa to 270 GPa to 220 GPa and demonstrated adhesion and fatigue strength enhancement during loading [24]. The lubricant additives are added to the nanocomposite coatings to improve the lubricity of the nanocomposite coatings at low and medium temperatures. The crystal of silver has a face-centered cubic structure, which occurs at the intergranular slip and has low shear stress. In addition, silver has good thermochemical stability, which allows it to act as a solid lubricant from room temperature (RT) to 500 °C. Ag is added to the nanocomposite coatings to improve the tribological properties of the nanocomposite coatings over a wide temperature range. The use of Ag-based Ag/TiB_x nanocomposite coatings embedded in extremely hard, wear-resistant stoichiometric TiB_x, along with the addition of Ag, which acts as a solid lubricant, decreases the CoF from 0.77 to 0.35, even at RT [25]. The incorporation of Ag contributes to a significant reduction in the CoF and wear rate at high temperatures below 500 °C, while the synergistic effect of the Ag distributed at grain boundaries and the outermost oxides dominated the excellent self-lubrication at 500–700 °C [26]. Therefore, Ag was doped into the γ-Fe_2O_3@SiO_2 nanocomposite to improve the wide range of tribological properties.

Therefore, Ag is applied to dope the γ-Fe_2O_3@SiO_2 nanocomposites, and the high-temperature tribological properties of Ag-doped γ-Fe_2O_3@SiO_2 nanocomposites are systematically investigated in the present paper. Sol-gel technology is useful for the preparation of the nanocomposites. Firstly, the Ag doping of γ-Fe_2O_3@SiO_2coatings was deposited on steel. Then, the tribological properties of the Ag-doping of γ-Fe_2O_3@SiO_2 coatings are studied from RT to 600 °C in the open air, and the high-temperature antifriction mechanism of γ-Fe_2O_3@SiO_2 nanocomposite coatings is also studied. It is necessary to prepare and investigate the tribological properties of γ-Fe_2O_3@SiO_2-Ag nanocomposite coatings and clarify the friction mechanism of the friction system over a wide temperature range. The tribological properties of the γ-Fe_2O_3@SiO_2-Ag nanocomposite coatings are investigated at the temperatures of RT, 100 °C, 300 °C, 500 °C, and 600 °C in ambient air, and understanding of the mechanism responsible for wide-temperature antifriction behaviors and the wear resistance of the nanocomposite coatings is also clarified. In this paper, the influence of Ag content on the tribological properties of γ-Fe_2O_3@SiO_2-Ag nanocomposite coatings from RT to 600 °C was studied, and the synergistic effect of Ag and oxides in the nanocomposite coatings was investigated. The experimental results are expected to provide a possible fundamental theory of soft metal-doped nanocomposite coatings for engineering applications under varied temperature conditions.

2. Experimental Details

2.1. Preparation of γ-Fe_2O_3@SiO_2-Ag Nanocomposite Coatings

The materials include: ferric nitrate ($Fe(NO_3)_3 \cdot 9H_2O$, 98.5 wt.%), tetraethyl orthosilicate (TEOS, 98%), and silver nitrate ($AgNO_3$, 99.8%). The solvents are ethanol (C_2H_6O, 99.7%) and distilled water. The catalytic agent is nitric acid (HNO_3, 69.2%). All the reactants and solvents used are of analytical grade in the present work.

2.1.1. Synthesis of the Sol

The experimental reagents are shown in Table 1. $AgNO_3$ provides the Ag precursor for the nanocomposites. Three groups of the nanocomposite coatings with different Ag contents were prepared, and the Ag content was 10 wt.%, 18 wt.%, and 24 wt.%, respectively. The γ-Fe_2O_3@SiO_2-Ag nanocomposite coatings with different Ag contents are denoted as 10 wt.%Ag, 18 wt.%Ag, and 24 wt.%Ag, respectively. $Fe(NO_3)_3 \cdot 9H_2O$ is dissolved into ethanol. TEOS is added and a glass rod is used to stir evenly, and then the catalyst of HNO_3 is added to adjust the PH of the solution to 2. After magnetic stirring for 8 h, $AgNO_3$ is added, and then the mixture is stirred for 2 h. A high-speed steel disc was placed on the turntable of the spray photoresist coating device by the rotating coating method, and the

turntable speed was set to 3000 rpm for 50 s. Then, the coated high-speed steel disc coating was left to stand for 1 day at RT, and heated in a constant temperature drying oven to 50 °C for 24 h and 80 °C for 6 h. The dried coatings were placed in a resistance furnace to heat at 100 °C for 1 h, 300 °C for 2 h, and 400 °C for 1 h. Finally, the γ-Fe_2O_3@SiO_2-Ag nanocomposite coatings were obtained.

Table 1. Reagents and the contents.

Number	Reagent	Parameter	The Mass Content of Ag/%
	TEOS	5 mL	
	$Fe(NO_3)_3 \cdot 9H_2O$	4.5283 g	
1		0.3847 g	10
2	$AgNO_3$	0.7692 g	18
3		1.1539 g	24
	EtoH	10 mL	

2.1.2. The Preparation of the Nanocomposite Coatings

The high-speed steel (HSS) is M2 steel. M2 steel is an 18% tungsten-based high-speed tool steel with high toughness, good cutting performance, excellent thermal hardness, wear resistance and heat treatment up to 70 HRC, and a high cobalt content that allows the steel to maintain hardness at high service temperatures. M2 high-speed steel has excellent thermal stability and is more suitable for high-temperature processing. High-speed tool steel is a tool steel containing high alloying elements, including carbon (C), silicon (Si), manganese (Mn), phosphorus (P), sulfur (S), chromium (Cr), molybdenum (Mo), cobalt (Co), vanadium (V), and other elements. Among them, C, Si, Mn, P, and S are classified as low-alloying elements, while Cr, Mo, Co, and V are high-alloying elements. HSS discs with a 30 mm diameter and a 5 mm thickness were selected as substrates. The sol was deposited onto the steel substrate surface by the Spray photoresist coating device (EVG101CS, EV Group, Sankt Florian am Inn, Austria). First, the sol was shaken for 10 min by an ultrasonic wave concussion machine (YL-31s, Kunshan Ultrasonic Instrument Co., Ltd., Kunshan, China). Then, the sol was dripped onto the surface of the steel. The steel substrate was then rotated at a speed of 3000 rpm for 50 s. After spin coating, the nanocomposite coatings were dried in the vacuum dry cabinet at a temperature of 50 °C and a heating rate of 5 °C min^{-1} for 4 h, 60 °C at a heating rate of 3 °C min^{-1} for 2 h, and 80 °C at a heating rate of 2 °C min^{-1} for 2 h, respectively. Then, the steel flats with the coatings were treated in the muffle furnace at 200 °C with a heating rate of 2 °C for 1 h and 400 °C at a heating rate of 3 °C for 2 h, respectively.

2.2. *Characterization of the γ-Fe_2O_3@SiO_2-Ag Nanocomposite*

The phase analyses and microstructures were conducted by X-ray diffractometry (XRD, D8-Advance, Bruker, Berlin, Germany). Cu-kα radiation (λ = 0.15406 nm) with a voltage of 60 kV, a power of 2.2 kW, and a current of 60 mA was utilized. The scan rate was 0.5° per second in the 2θ range of 10°~90°. The morphology and element compositions of the nanocomposite coatings were examined using scanning electron microscopy (SEM) (S-3000N, HITACHI, Chiyoda City, Japan). Raman spectroscopy (HR800, HORIBA JobinYvon, Paris, France) was used to measure the microstructure of the nanocomposite coatings using a laser with a wavelength of 532 nm in the range of 250~3000 cm^{-1}. Fourier transform infrared spectrometry (FTIR) (Nicolet iS50, Thermo Fisher, Waltham, MA, USA) was performed for the synthesized nanocomposite gel in the range of 400~2800 cm^{-1}.

2.3. Tribotest of γ-Fe$_2$O$_3$@SiO$_2$-Ag Nanocomposite Coatings

The friction and wear performances were estimated by a Rtec high-temperature rotary ball-on-disc configuration tribometer from RT to 600 °C in ambient air. The temperatures were RT to 600 °C, which is the highest temperature of most moving machine parts for aerospace. ZrO$_2$ balls with diameters of 9.5 mm were used as the friction pairs. Before tribotests, the disc and ball were both cleaned with ethanol for 3 min and dried in the vacuum dry cabinet. The rotating flats were heated to the set temperatures and then kept at a constant temperature during sliding. The sliding time, speed, and load were 30 min, 0.05 m/s and 2 N, respectively. The sliding time was 30 min. For characteristics or descriptions of friction, a dimensionless quantity called the CoF is used. The CoF is defined as the ratio of the friction force to the normal force that acts perpendicularly to the two surfaces in contact. In order to measure the CoF, one surface is brought into contact with another and moved relative to it. When the two surfaces are in contact, the perpendicular force is defined as the normal force N. The tangential friction force F is the force that opposes the relative movement between the two surfaces. From Amonton's law, the CoF is defined as the ratio of the friction force to the normal force. To evaluate the friction and wear performances of the friction system, a friction experiment was then conducted by using a pin-on-disk tribometer with a rotary drive. The wear tests were executed by means of a ball-on-disk wear tester. The wear tests were tested three times for each group to reduce the plagiarism percentage. The topography of wear tracks on the sample and the sphere was measured. The wear track of the sample is of a cylindrical shape and the shape of the wear scar of the ball depends on the tested material. The wear volume of the sphere was calculated by means of the ASTM699-95 formula and presented for different combinations of the contact ball and coatings [27]. After friction tests, the wear surface on the disk of tested samples after tribological tests was scanned with SEM in order to evaluate the wear properties of the γ-Fe$_2$O$_3$@SiO$_2$-Ag nanocomposite coating at different temperatures. XRD and Raman were used to obtain the microstructure of the worn surfaces of the disk.

The Vickers microhardness tester is used to test the hardness of the sample. The load is 0.98 g and the loading time is 15 s. Five points are selected for testing, and the average value is calculated as the hardness of the sample. The spacing between the test points is about 5 mm. The average hardness of each sample obtained by calculating the average value of five test points is calculated.

3. Results and Discussion

3.1. Microstructure of γ-Fe$_2$O$_3$@SiO$_2$-Ag Nanocomposite Coatings

3.1.1. XRD Measurements

Figure 1 shows the XRD microstructures of γ-Fe$_2$O$_3$@SiO$_2$-Ag nanocomposite coatings with different Ag contents. It is shown in Figure 1 that the nanocomposite coatings with different Ag contents contain γ-Fe$_2$O$_3$, Ag, and amorphous SiO$_2$. The diffraction peaks of 18 wt.%Ag and 24 wt.%Ag coatings become sharp, indicating that the increase in Ag content is conducive to the enhancement of Ag crystallinity. According to Scherrer's formula, the average particle sizes of γ-Fe$_2$O$_3$ in 10 wt.%Ag, 18 wt.%Ag, and 24 wt.%Ag coatings are 13.47 nm, 14.68 nm, and 14.42 nm, respectively [28]. The average particle size of γ-Fe$_2$O$_3$ in the nanocomposite coating is 14.15 nm, which shows that Ag doping does not affect the particle size of γ-Fe$_2$O$_3$.
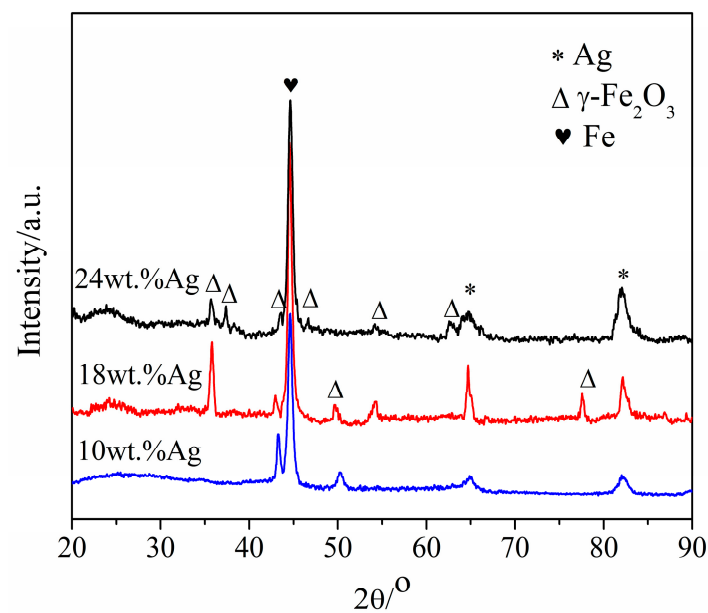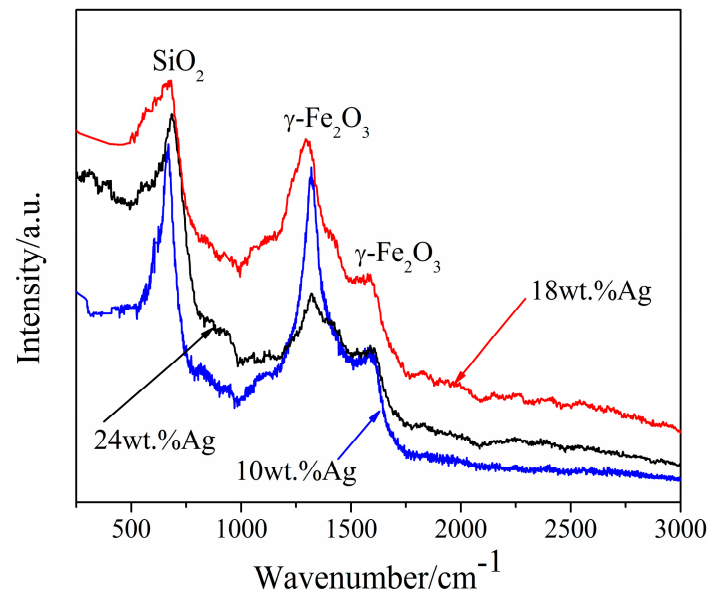
Figure 1. XRD patterns of the nanocomposite coatings with different Ag contents.

3.1.2. Raman Measurements

Figure 2 shows the Raman spectra of the nanocomposite coatings with different Ag contents. Since Ag is a phase, there is no characteristic peak of Ag in the Raman spectra. The Raman spectra show that no new substance is generated in the nanocomposite coatings with different Ag contents.
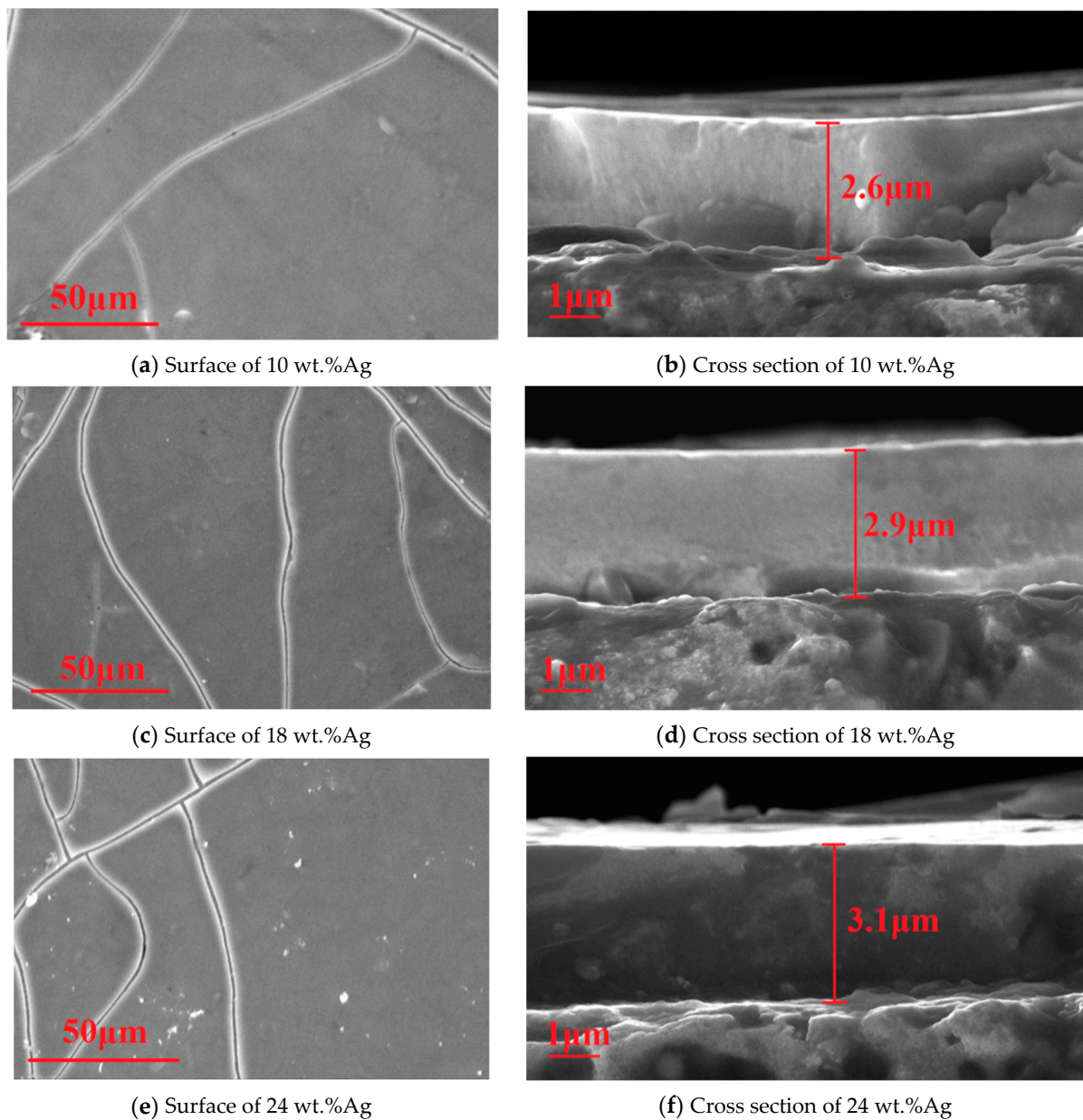

Figure 2. Raman patterns of the nanocomposite coatings with different Ag contents.

3.1.3. SEM

Figure 3 shows the SEM images of the surface and cross-sections of γ-Fe$_2$O$_3$@SiO$_2$-Ag nanocomposite coatings with different Ag contents. It can be seen from Figure 3 that the surface of the nanocomposite coatings with different Ag contents is relatively flat but there are weak cracks in the coatings. It is shown from the cross-section SEM image that the thicknesses of three coatings slightly increase with the increase in Ag content, which is 2.6 µm, 2.9 µm, and 3.1 µm, respectively. The bonding surface between the coating and the substrate formed by 10 wt.%Ag and 18 wt.%Ag coatings is loose, and there are a few holes

and voids at the interface. The internal structure of 24 wt.%Ag is relatively dense, and the combination with the substrate is also the closest.

(**a**) Surface of 10 wt.%Ag

(**b**) Cross section of 10 wt.%Ag

(**c**) Surface of 18 wt.%Ag

(**d**) Cross section of 18 wt.%Ag

(**e**) Surface of 24 wt.%Ag

(**f**) Cross section of 24 wt.%Ag

Figure 3. SEM images of the surface and cross-sections of the nanocomposite coatings with different Ag contents.

3.1.4. Hardness of γ-Fe$_2$O$_3$@SiO$_2$-Ag Nanocomposite Coatings

The microhardnesses of the nanocomposite coatings with different Ag contents are shown in Table 2. The microhardnesses of the nanocomposite coatings decrease first and then increase slightly with the increase in Ag content. This is because Ag is soft, which reduces the microhardness of the nanocomposite coatings. However, it is interesting that the hardness of the nanocomposite coatings with 24 wt.%Ag increases slightly because the coating microstructure is dense and bonds well with the substrate according to the SEM cross-section.

Table 2. The microhardness of the nanocomposite coatings with different Ag contents.

Ag Content	Hardness (HV)
10 wt.%Ag	577
18 wt.%Ag	493
24 wt.%Ag	547

3.2. Tribological Properties of γ-Fe₂O₃@SiO₂-Ag Nanocomposite Coatings

The tribological experiments of γ-Fe$_2$O$_3$@SiO$_2$-Ag nanocomposite coatings were carried out at RT, 100 °C, 300 °C, 500 °C, and 600 °C, respectively, to investigate the tribological properties of nanocomposite coatings with different Ag contents over a wide range of temperatures. After the tribological experiments, the worn surface morphology and compositions of the nanocomposite coatings were observed and analyzed, and the wide-temperature lubrication mechanism of the nanocomposite coatings was discussed.

3.2.1. Room Temperature

1. CoF

Figure 4 shows the CoF of the γ-Fe$_2$O$_3$@SiO$_2$-Ag nanocomposite coatings with different Ag contents at RT. It is shown in Figure 4 that the CoF curves of each coating are relatively stable with time, and the initial CoF of 10 wt.%Ag is low compared to that of the γ-Fe$_2$O$_3$@SiO$_2$ nanocomposite coatings. The CoF is about 0.45 and finally stabilized, which is slightly higher than the stable CoF of γ-Fe$_2$O$_3$@SiO$_2$ nanocomposite coatings (about 0.35), possibly due to the low amount of Ag doping, which is not completely covered on the worn surface during the friction process and cannot play an effective role in the antifriction behaviors of the nanocomposite coatings. The CoF curves of the 18 wt.%Ag and 24 wt.%Ag of γ-Fe$_2$O$_3$@SiO$_2$-Ag nanocomposite coatings decreased slowly with time, and finally, the CoFs stabilized at about 0.3 and 0.25, respectively, which were lower values than those of the nanocomposite coatings without Ag. The experimental results show that the CoF of the nanocomposite coatings containing Ag decreases with the increase in Ag content, and the doping of Ag reduces the CoF of the nanocomposite coatings at RT within a certain range.
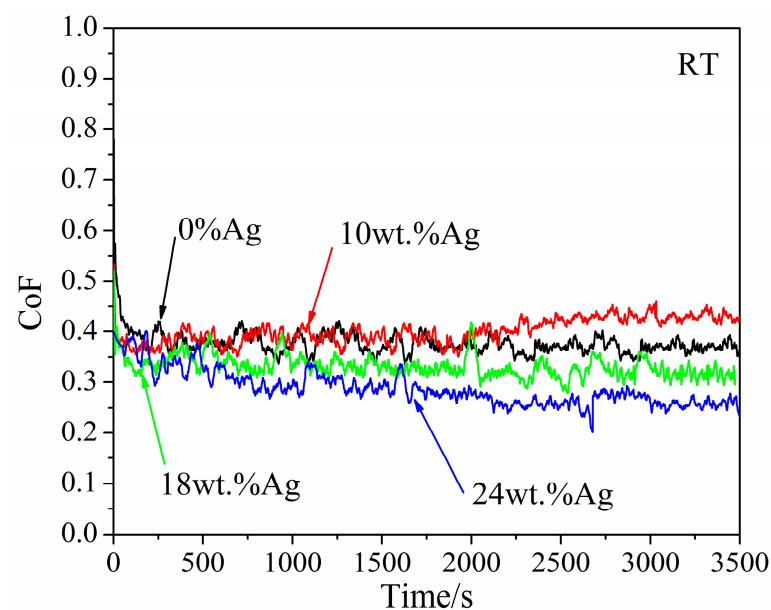
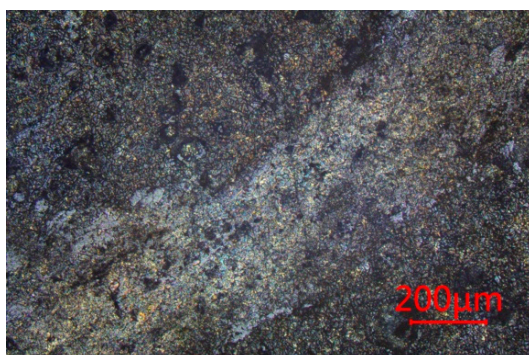**Figure 4.** CoF of the nanocomposite coatings with different Ag contents at RT.

2.   Wear rate

Figure 5 shows the volume wear rate of the γ-Fe_2O_3@SiO_2-Ag nanocomposite coatings with different Ag contents at RT. The volume wear rate decreases with the increase in Ag content. The volume wear rates of 18 wt.%Ag and 24 wt.%Ag nanocomposite coatings are lower than those of γ-Fe_2O_3@SiO_2 nanocomposite coatings, which are 0.71×10^{-5} mm^3/(Nm) and 0.26×10^{-5} mm^3/(Nm), respectively.
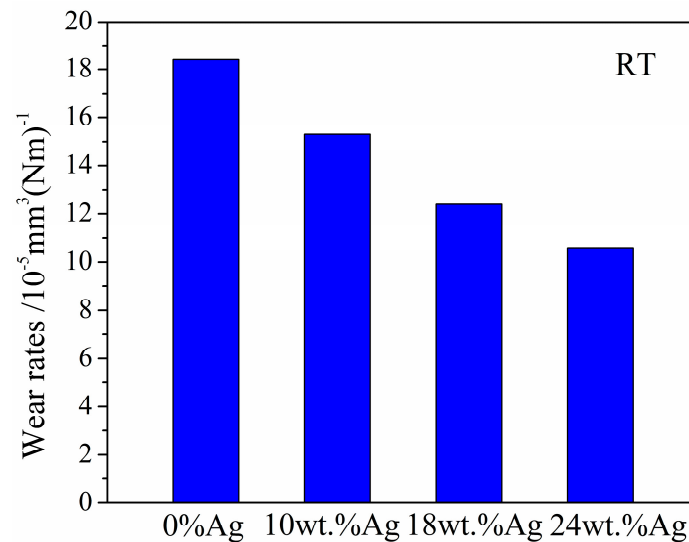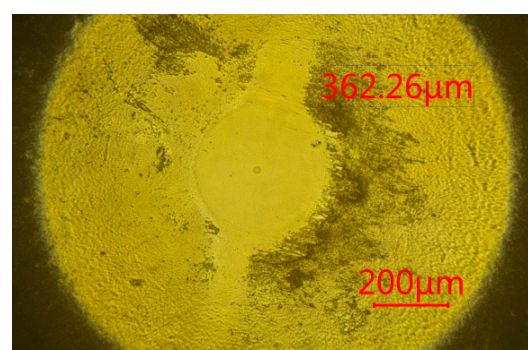

Figure 5. The volume wear rate of the nanocomposite coatings with different Ag contents at RT.

Figure 6 shows the worn surface morphology of the nanocomposite coatings with different Ag contents and the ball at RT. The worn surface of 10 wt.%Ag nanocomposite coatings exhibits abrasive wear and is covered by a layer of film. The transferred films are brittle and show poor bonding forces with the substrate, which are peeled continuously during sliding.

The surface of the nanocomposite coatings has obvious pits due to spalling, and coating chips are present around the worn surface of the ball. The brittle surface fracture of 18 wt.%Ag and 24 wt.%Ag coatings is serious, and the fracture cracks are expanded, resulting in flake spalling in the nanocomposite coatings. The wear mechanism of the nanocomposite coatings is brittle fracture and peeling wear, and the diameters of the wear spots on the ball are small.
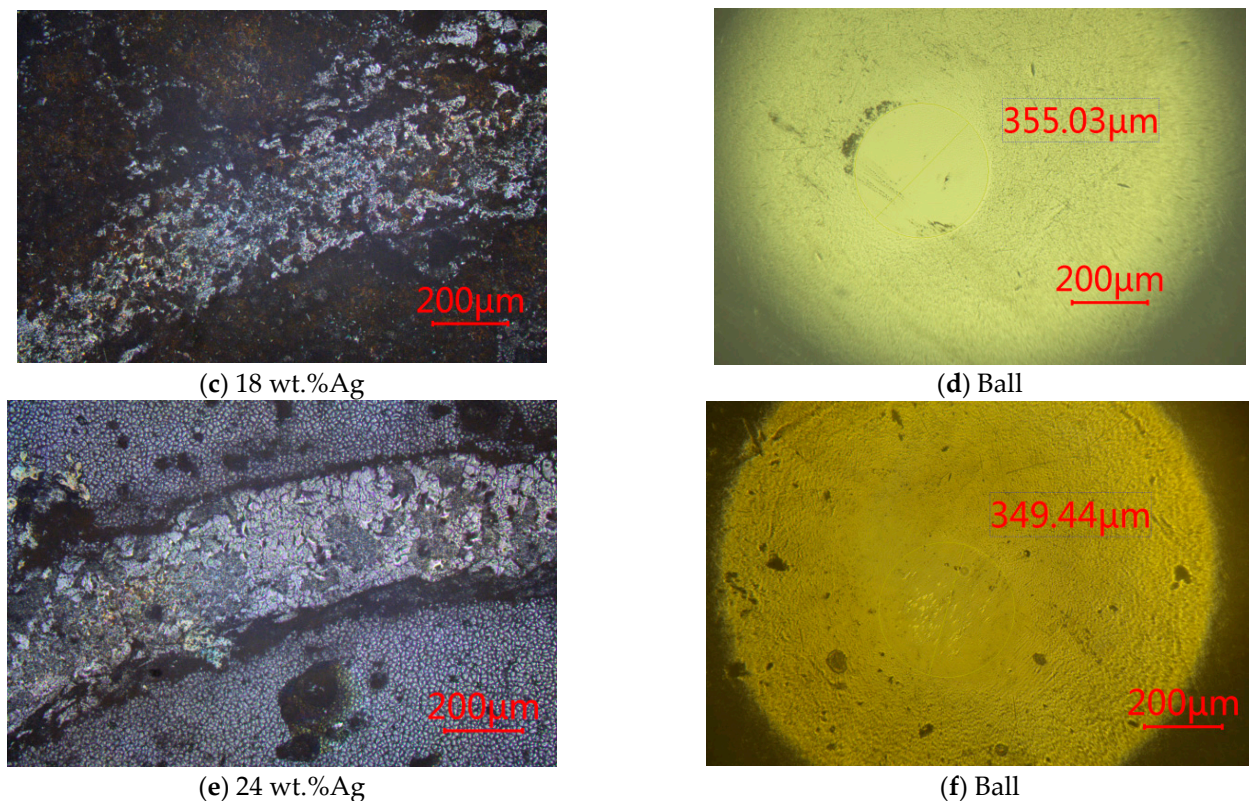

(**a**) 10 wt.%Ag

(**b**) Ball

Figure 6. *Cont.*

(**c**) 18 wt.%Ag

(**d**) Ball

(**e**) 24 wt.%Ag

(**f**) Ball

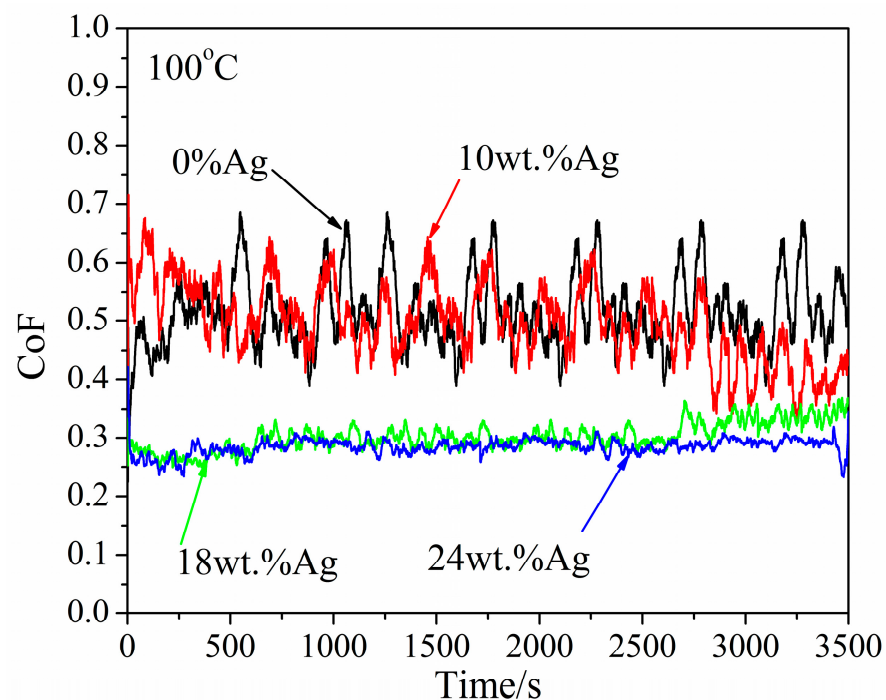**Figure 6.** The worn surface of the nanocomposite coatings with different Ag contents and the ball at RT.

3.2.2. At 100 °C

1.   CoF

Figure 7 shows the CoF curves of the γ-Fe_2O_3@SiO_2-Ag nanocomposite coatings with different Ag contents at 100 °C. It is found that the average CoF of 10 wt.%Ag, 18 wt.%Ag, and 24 wt.%Ag nanocomposite coatings are 0.45, 0.3, and 0.25, respectively. The CoF curve of 10 wt.%Ag nanocomposite coatings fluctuates between 0.35 and 0.45, indicating that the surface of the nanocomposite coatings with a low Ag content was not completely covered by the Ag films. Under the action of temperature and friction, oxides existing on the worn surface of the nanocomposite coatings were peeled off from the worn surface of the nanocomposite coatings acting as abrasive particles. However, the CoFs of 18 wt.%Ag and 24 wt.%Ag nanocomposite coatings were stable, and the CoF of 18 wt.%Ag was also stable at about 0.25 in the initial stage, although it increased slowly after 2100 s and the CoF of 24 wt.%Ag was stable at about 0.25. This shows that Ag was slowly diffused to the worn surface, forming a tribological transferred film, and Ag in the worn surface was supplemented by the nanocomposite coatings, which played an effective anti-friction role during the friction process.

2.   Wear rate

Figure 8 shows the volume wear rates of the γ-Fe_2O_3@SiO_2-Ag nanocomposite coatings with different Ag contents at 100 °C. It is found that the volume wear rates of 10 wt.%Ag, 18 wt.%Ag, and 24 wt.%Ag nanocomposite coatings were 6.85×10^{-5} mm^3/(Nm), 0.64×10^{-5} mm^3/(Nm), and 0.57×10^{-5} mm^3/(Nm), respectively. The volume wear rate of nanocomposite coatings with different Ag contents is lower than that of the undoped Ag nanocomposite coatings. In particular, 18 wt.%Ag and 24 wt.%Ag nanocomposite coatings show good wear resistance.

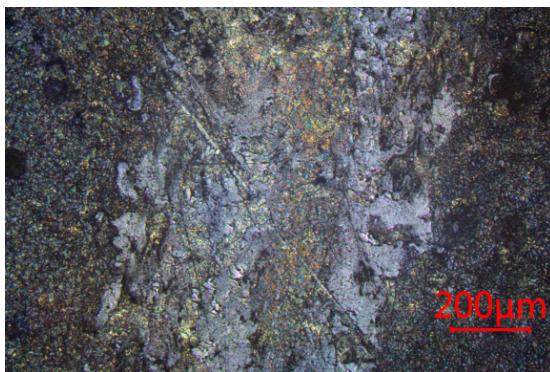**Figure 7.** CoF of the nanocomposite coatings with different Ag contents at 100 °C.
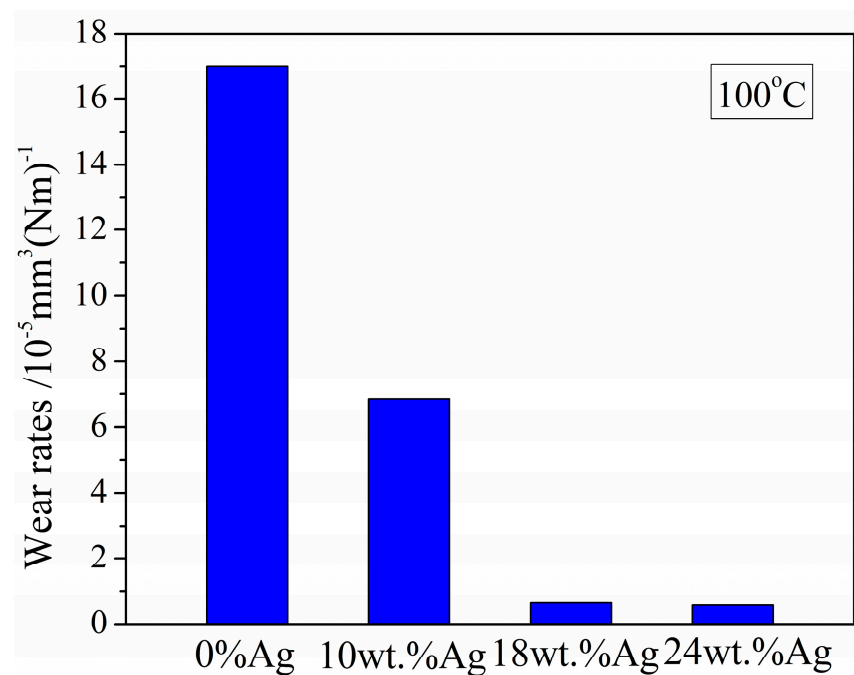
Figure 8. The volume wear rate of the nanocomposite coatings with different Ag contents at 100 °C.

Figure 9 shows the surface morphology of the nanocomposite coatings with different Ag contents at 100 °C. The 10 wt.%Ag nanocomposite coatings show obvious wear particles, uneven wear, and abrasive debris around the ball. Therefore, the CoF curve fluctuates greatly. The wear width of 18 wt.%Ag nanocomposite coatings is small compared with 10 wt.%Ag. The wear mechanism is mainly abrasive wear and the transfer films of the coatings on the wear scar of the ball, which explain the increase in the CoF of the nanocomposite coatings during the period of friction and wear experiments. Continuous lubrication films appear on the worn surface of 24 wt.%Ag, and there are abrasive particles on the worn surface. The wear mechanism is mainly abrasive wear. The diameter of the worn
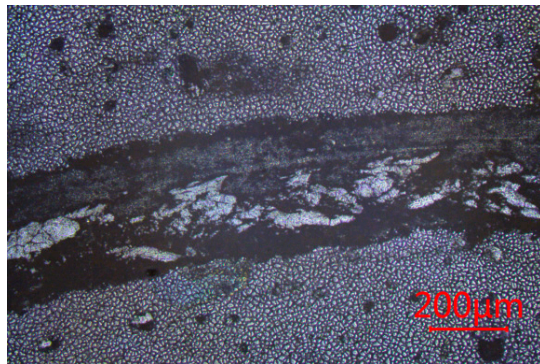
surface of the ball is small and there are transfer films distributed on the worn surface of the ball.
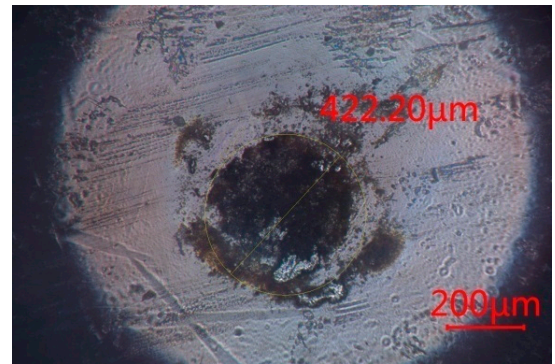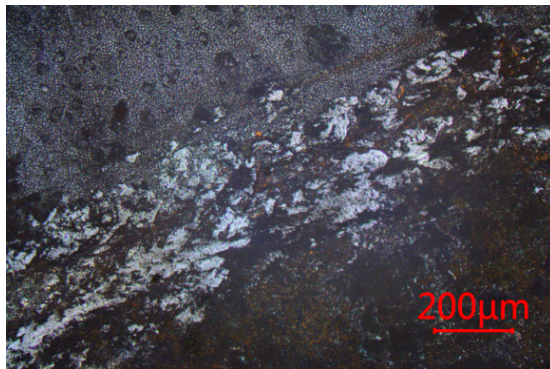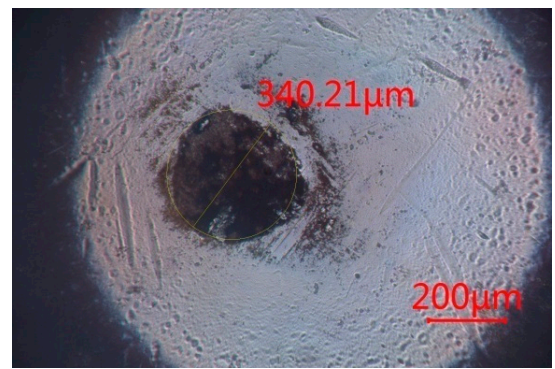

(**a**) 10 wt.%Ag
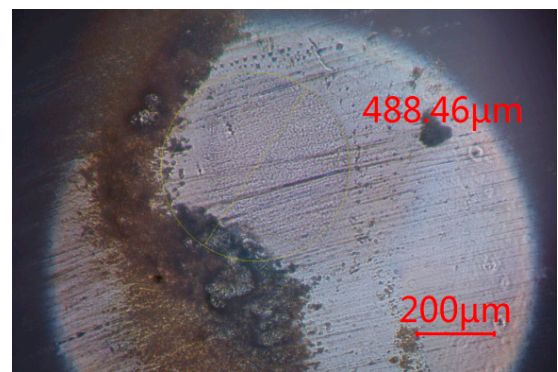
(**b**) Ball

(**c**) 18 wt.%Ag

(**d**) Ball

(**e**) 24 wt.%Ag

(**f**) Ball
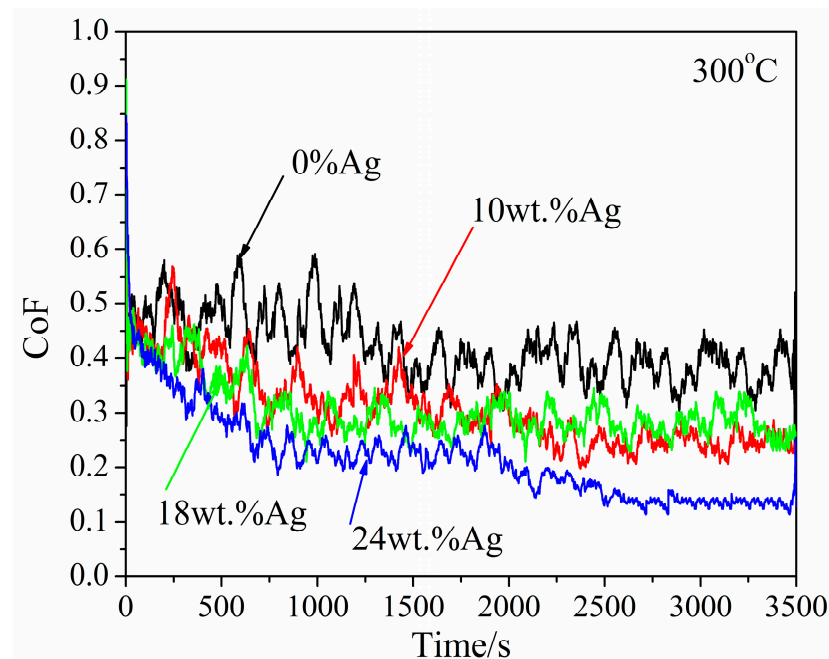
Figure 9. The worn surface of the nanocomposite coatings with different Ag contents and the ball at 100 °C.

3.2.3. At 300 °C

1. CoF

Figure 10 shows the CoF of the nanocomposite coatings with different Ag contents with the sliding time at 300 °C. It is found that the stable CoF of the nanocomposite coatings with Ag contents is low compared with that of the nanocomposite coatings without Ag. After a period of run-in, the CoF of each coating reaches a relatively stable value. Among them, the CoF curve of 10 wt.%Ag nanocomposite coatings fluctuates. The stable CoF of 24 wt.%Ag nanocomposite coatings is about 0.18. At this temperature, the CoF curves of 18 wt.%Ag and 24 wt.%Ag nanocomposite coatings are relatively stable. The diffusion of Ag becomes fast from the inside to the top surface of the nanocomposite coatings. This

is because Ag increased with the increase in temperature. However, the surface hardness of the coatings decreases because Ag was diffused to the top surface. The initial CoFs of 18 wt.%Ag and 24 wt.%Ag nanocomposite coatings are high. The worn surface is gradually compacted after deformation, and the CoF curve of 18 wt.%Ag and 24 wt.%Ag declines gradually during the progress of the friction and wear. Finally, the stable CoF is lower than that at 100 °C.

Figure 10. CoF of the nanocomposite coatings with different Ag contents at 300 °C.

2. Wear rate

Figure 11 shows the volume wear rates of the nanocomposite coatings with different Ag contents at 300 °C. It is shown that the volume wear rates of 10 wt.%Ag, 18 wt.%Ag, and 24 wt.%Ag nanocomposite coatings are 12.5×10^{-5} mm^3/(Nm), 11.8×10^{-5} mm^3/(Nm), and 5.65×10^{-5} mm^3/(Nm), respectively. The volume wear rate of each nanocomposite coating decreases gradually, but the volume wear rate of the nanocomposite coatings is high because there is more Ag formed on the worn surface. The friction and deformation first occur on the Ag lubrication films due to the low surface strength of the nanocomposite coatings. Ag is partially worn off to stick to the ball with the increase in temperature. There are more obvious transfer films at this high temperature. Therefore, the worn surface is seriously accelerated due to the formation of adhesion, resulting in an increase in the amount of wear during the friction and wear.

Figure 12 shows the surface morphology of the nanocomposite coatings with different Ag contents at 300 °C. Discontinuous lubrication films were formed on the worn surface of 10 wt.%Ag and 18 wt.%Ag nanocomposite coatings. The lubrication films of 10 wt.%Ag were serious compared to 18 wt.%Ag nanocomposite coatings. At 24 wt.%Ag of the nanocomposite coatings, the wear scar width of the nanocomposite coatings became small, the lubricating films formed on the worn surface of the nanocomposite coatings were more continuous and dense, and there was micro-cutting on the worn surface. The transfer films on the worn surface of the ball were observed for the nanocomposite coatings with different Ag contents, and the diameters of the ball gradually decreased with the increase in Ag.
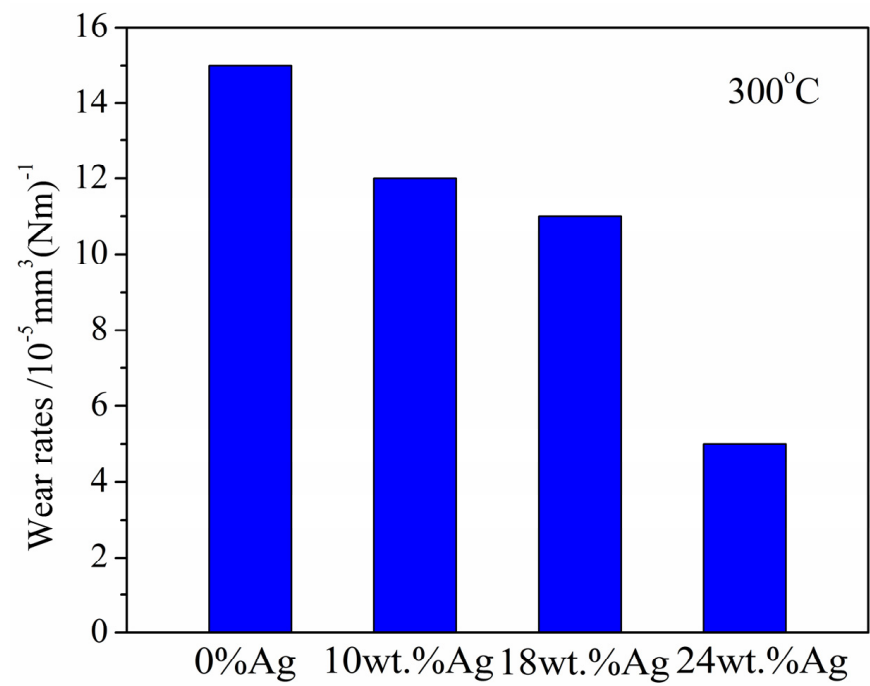
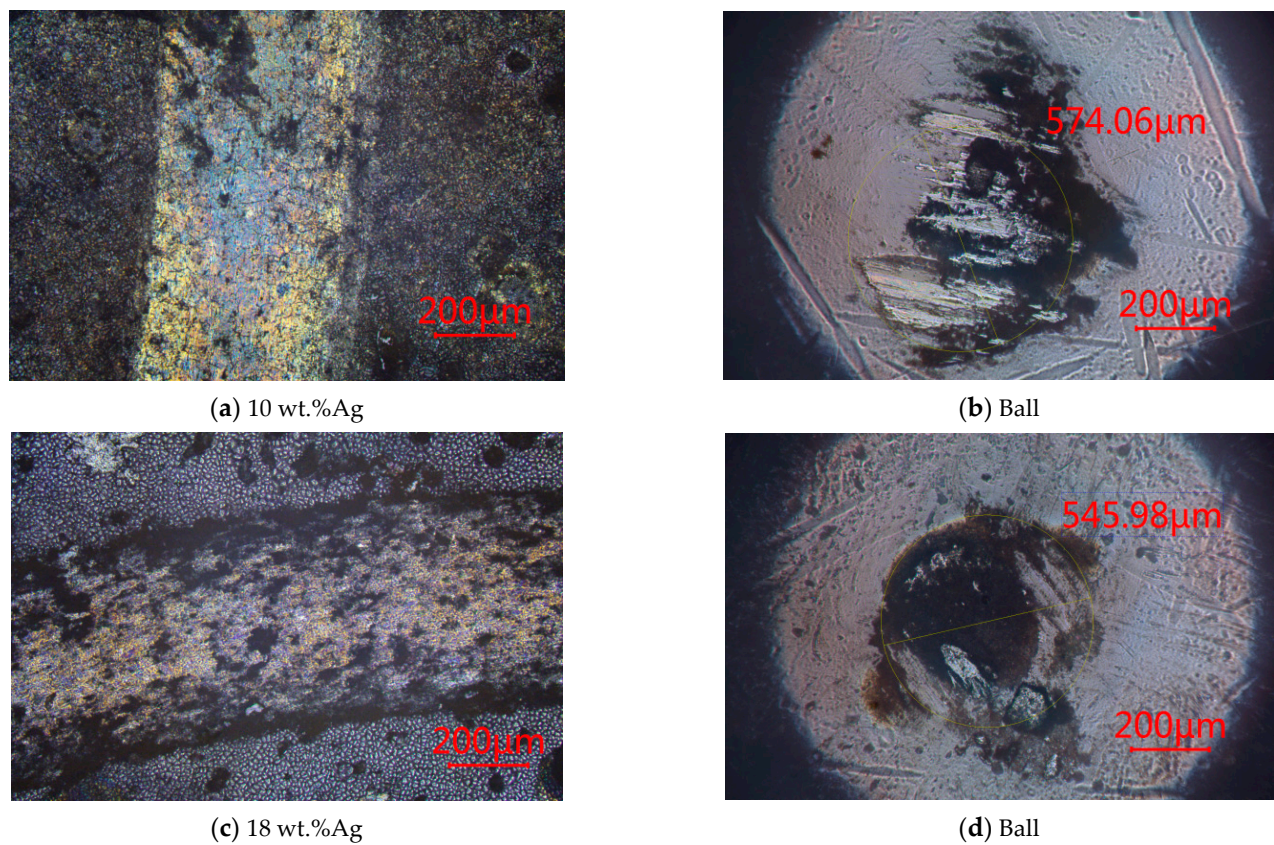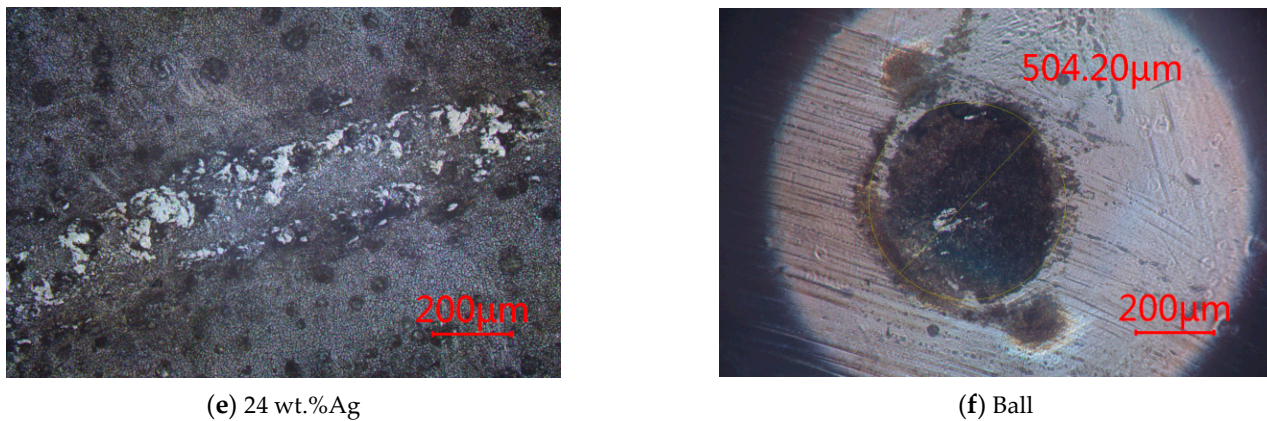**Figure 11.** The volume wear rate of the nanocomposite coatings with different Ag contents at 300 °C.

(**a**) 10 wt.%Ag

(**b**) Ball

(**c**) 18 wt.%Ag

(**d**) Ball

Figure 12. *Cont.*

(**e**) 24 wt.%Ag

(**f**) Ball

Figure 12. The worn surface of the nanocomposite coatings with different Ag contents and the ball at 300 °C.

3.2.4. At 500 °C

1. CoF

Figure 13 shows the CoF of the nanocomposite coatings with different Ag contents with the sliding time at 500 °C. It is shown that the CoF curve of the nanocomposite coatings with different Ag contents has a similar trend, which decreases slowly with time and finally stabilizes at a certain CoF value. The CoFs of 10 wt.%Ag of the nanocomposite coatings, 18 wt.%Ag of the nanocomposite coatings, and 24 wt.%Ag of the nanocomposite coatings are 0.08, 0.05, and 0.06, respectively. The running-in time of 18 wt.%Ag of the nanocomposite coatings is 2000 s, and the CoF is about 0.05 at the stable stage, while the initial CoF of 24 wt.%Ag is the lowest, and the CoF is about 0.06 after the running-in period of about 1500 s. The CoF of 10 wt.%Ag reaches a minimum value of about 0.08 after the running-in period of about 1800 s, and then increases slowly. The reason for the long running-in time of the nanocomposite coatings with different Ag contents is mainly due to the softness of γ-Fe_2O_3 and Ag, which reduces the surface hardness of the nanocomposite coatings, and the hardness differences between the substrate and the coatings become high and result in a large initial CoF. However, γ-Fe_2O_3 and Ag are transferred to the worn surface of the ball, and the worn surface is covered by a lubricating film during the friction process. γ-Fe_2O_3 has low shear performance and plays a synergistic lubricating role with Ag in the nanocomposite coatings. The CoF of the nanocomposite coatings with different Ag contents is as low as 0.1.

2. Wear rate

Figure 14 shows the volume wear rates of the nanocomposite coatings with different Ag contents at 500 °C. The volume wear rates of 10 wt.%Ag, 18 wt.%Ag, and 24 wt.%Ag of the nanocomposite coatings are 6.47×10^{-5} mm^3/(Nm), 8.54×10^{-5} mm^3/(Nm), and 4.32×10^{-5} mm^3/(Nm), respectively. The volume wear rate of the nanocomposite coatings containing Ag is low compared with the coatings without Ag, and the wear volume increases slightly first and then decreases with the increase in Ag content.

Figure 15 shows the wear morphology of the nanocomposite coatings with different Ag contents at 500 °C. At 500 °C, relatively continuous and dense lubricating films appear on the worn surfaces of 10 wt.%Ag, 18 wt.%Ag, and 24 wt.%Ag nanocomposite coatings. The abrasive surface of 10 wt.%Ag nanocomposite coatings has a microscopic cutting effect, which has a significant transferred film of the coating materials on the grinding ball spots. There are furrows on the worn surface of the 18 wt.%Ag nanocomposite coating, which has a high diameter to the ball and discontinuous distribution of the coating materials on the worn surface of the ball. The lubrication films on the worn marks of 24 wt.%Ag nanocomposite coatings are the smoothest, and there is only a small amount of wear debris on the worn surface. The wear mechanism is adhesive wear, and the transfer films are

distributed continuously on the wear scar of the ball. With the increase in Ag content, the lubrication films on the worn surface become continuous, which reduces the CoF of the nanocomposite coatings at 500 °C, and the diameters of the worn surface on the ball become small.
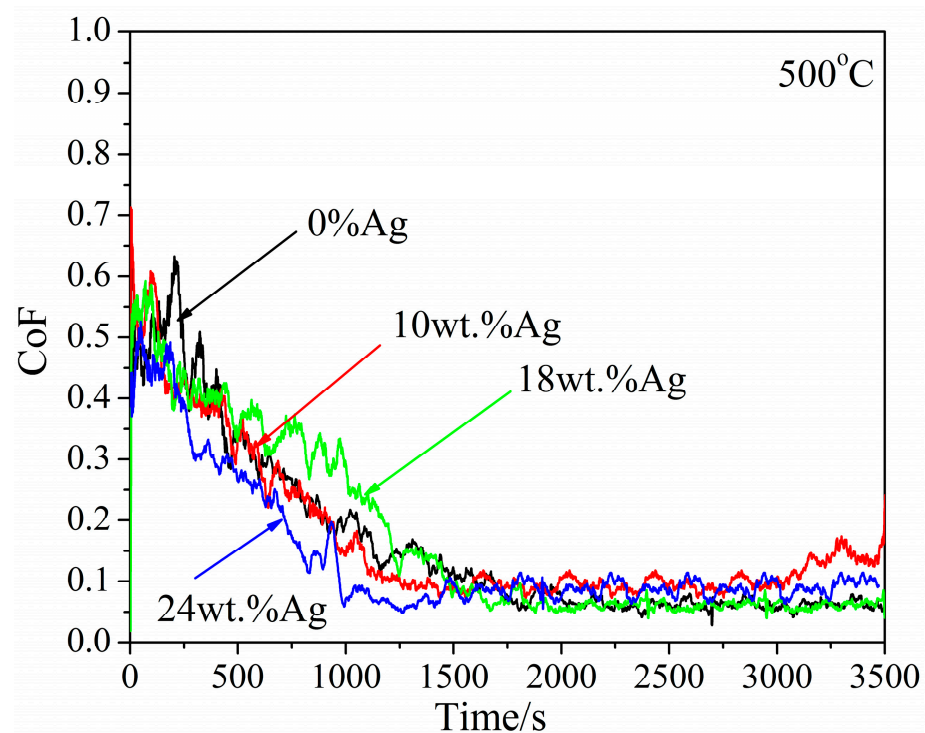

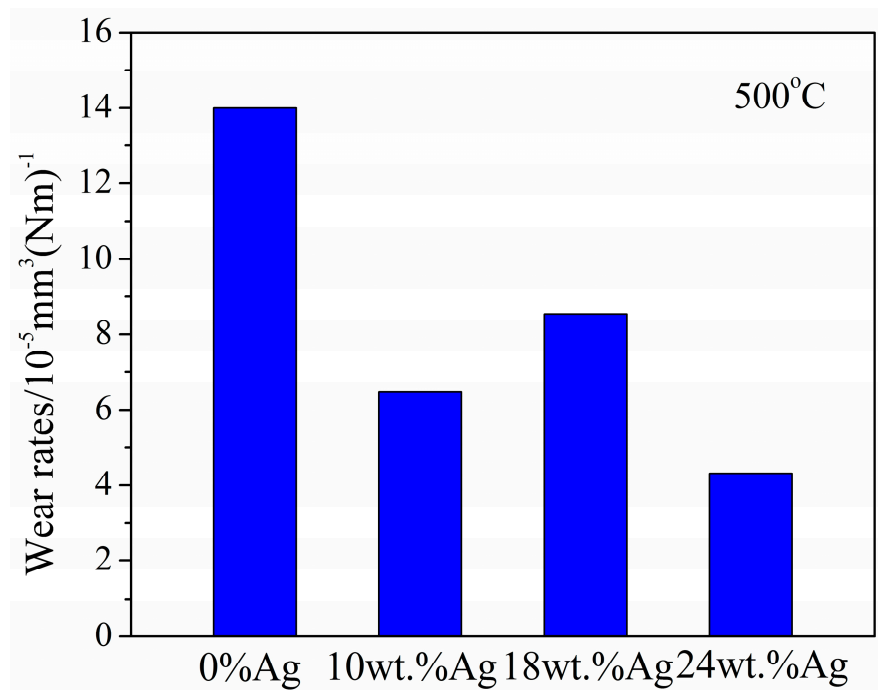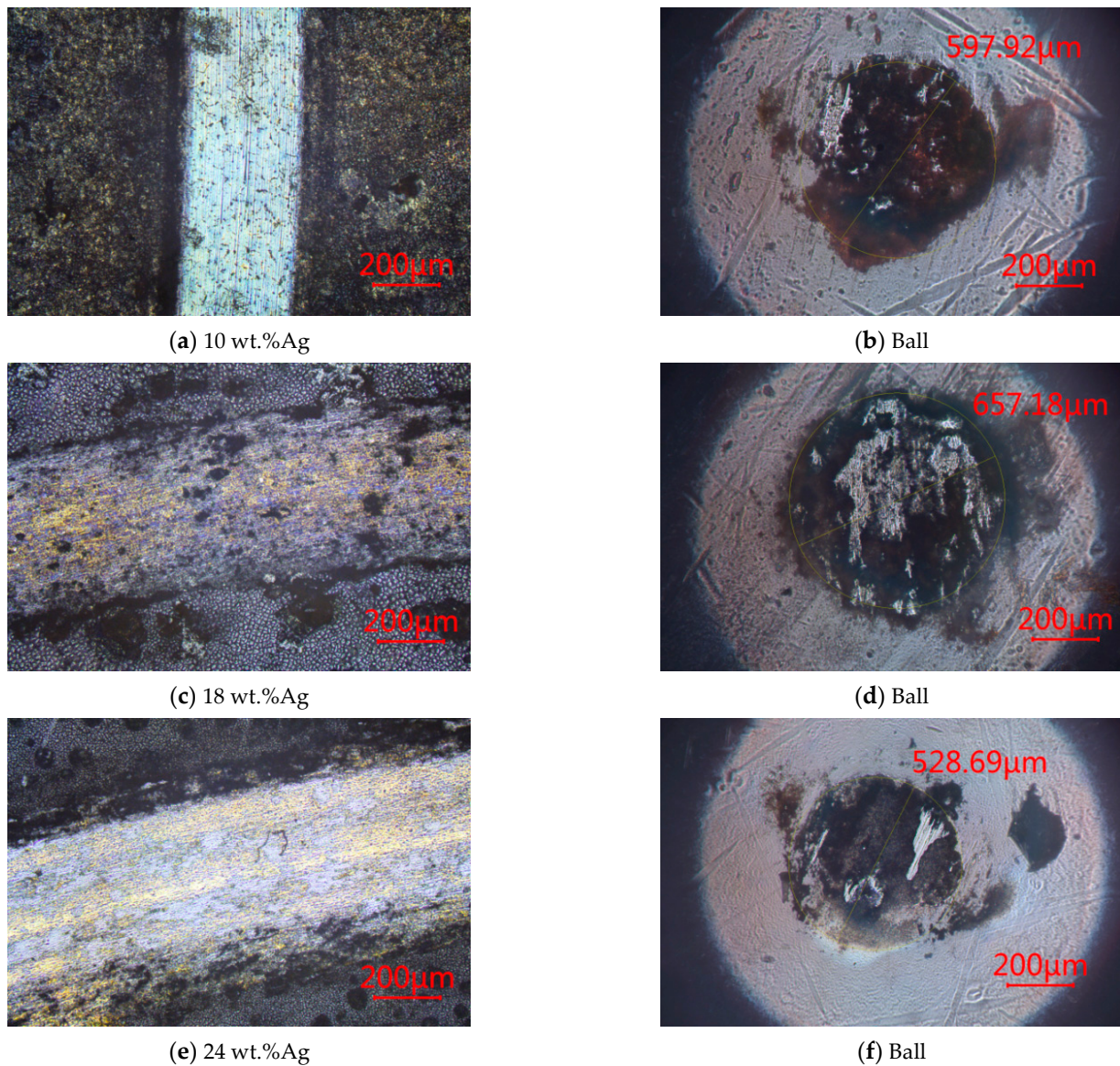**Figure 13.** CoF of the nanocomposite coatings with different Ag contents at 500 °C.

Figure 14. The volume wear rate of the nanocomposite coatings with different Ag contents at 500 °C.

(**a**) 10 wt.%Ag

(**b**) Ball

(**c**) 18 wt.%Ag

(**d**) Ball

(**e**) 24 wt.%Ag

(**f**) Ball

Figure 15. The worn surface of the nanocomposite coatings with different Ag contents and the ball at 500 °C.

3.2.5. At 600 °C

1.   CoF

Figure 16 shows the CoF of the nanocomposite coatings with different Ag contents with time at 600 °C. The stable CoF of the nanocomposite coatings doped with Ag is low compared to that of coatings without Ag. The CoF curve of 10 wt.%Ag fluctuates with the trend of decreasing first and then becoming stable. The CoF is stable at about 0.1. The initial CoF of 18 wt.%Ag is stable at about 0.15 after about 0.5, and the initial CoF of 24 wt.%Ag is about 0.3 and then becomes stable at about 0.05. The minimum CoF of the nanocomposite coatings at 600 °C is slightly high, which is attributed to the phase transition of some γ-Fe_2O_3 in the nanocomposite coating at this temperature.
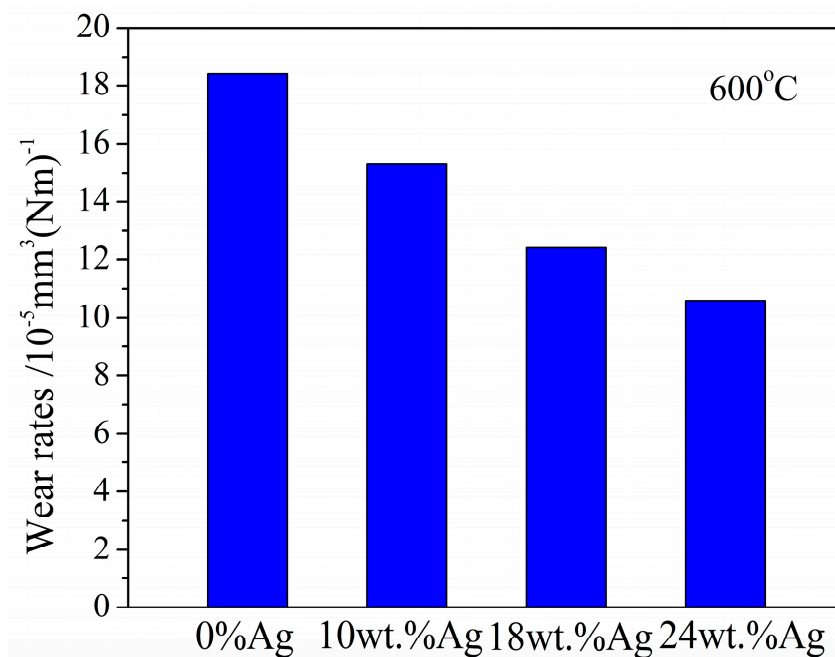
2.   Wear rate

Figure 17 shows the volume wear rates of the nanocomposite coatings with different Ag contents at 600 °C. The volume wear rates of 10 wt.%Ag, 18 wt.%Ag, and 24 wt.%Ag nanocomposite coatings are 15.4×10^{-5} mm^3/(Nm), 12.6×10^{-5} mm^3/(Nm), and 10.3×10^{-5} mm^3/(Nm), respectively. With the increase in Ag content, the volume

wear rate of the nanocomposite coatings decreases gradually, showing the anti-wear performances, but the volume wear rate increases slightly compared with that at 500 °C.
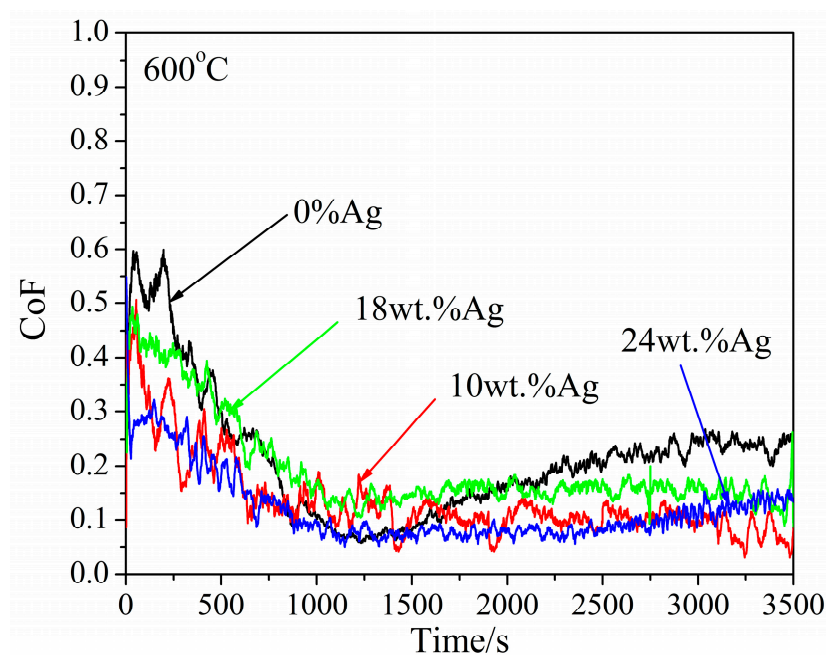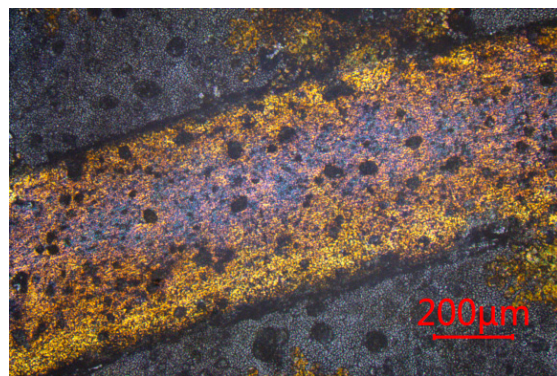

Figure 16. CoF of the nanocomposite coatings with different Ag contents at 600 °C.
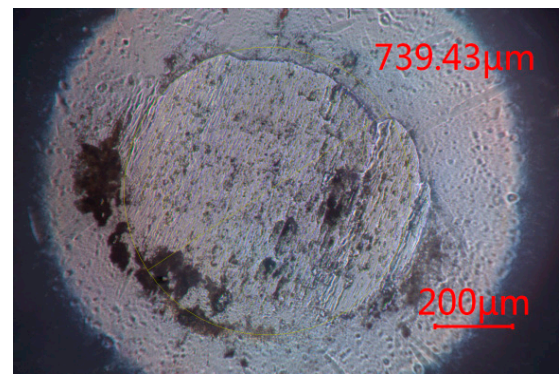

Figure 17. The volume wear rate of the nanocomposite coatings with different Ag contents at 600 °C.
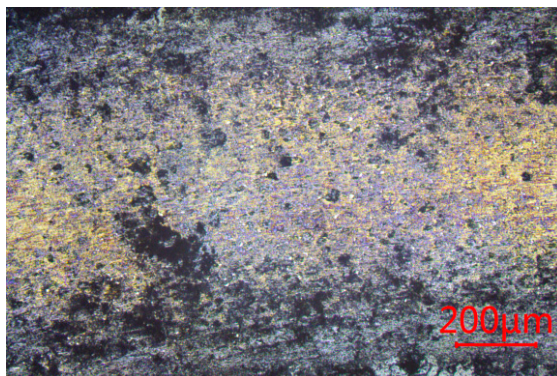
Figure 18 shows the wear morphology of the nanocomposite coatings with different Ag contents at 600 °C. There are micro-furrowing and slight pits on the worn surface of 10 wt.%Ag nanocomposite coatings. The wear mechanism is mainly abrasive wear, and the wear scar width of 18 wt.%Ag nanocomposite coatings is the widest. There is a relatively continuous lubrication film on the worn surface and slight peeling. The wear mechanism is mainly peeling wear, a furrow appears inside the 24 wt.%Ag wear, and the ball is worn through and failed. The diameter of the wear scar on each pair of balls is large, and a small amount of the coating materials are transferred to the wear scar on the ball.
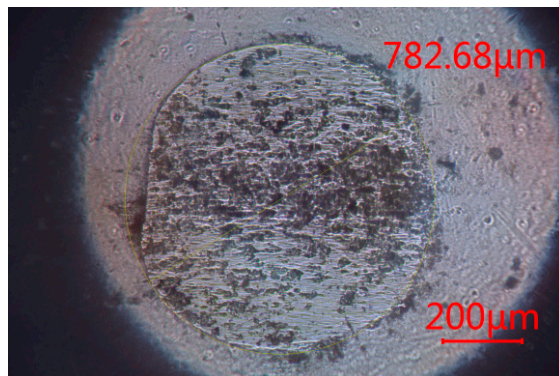
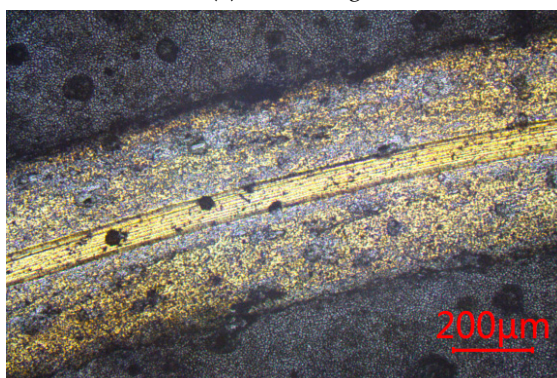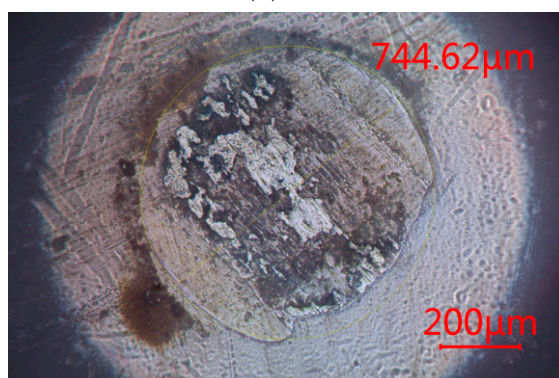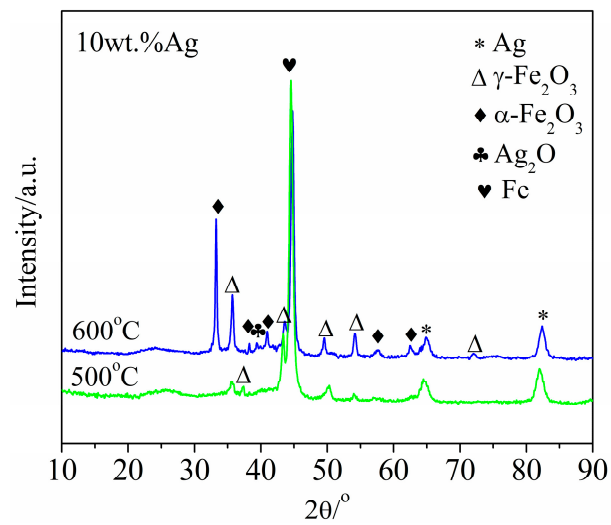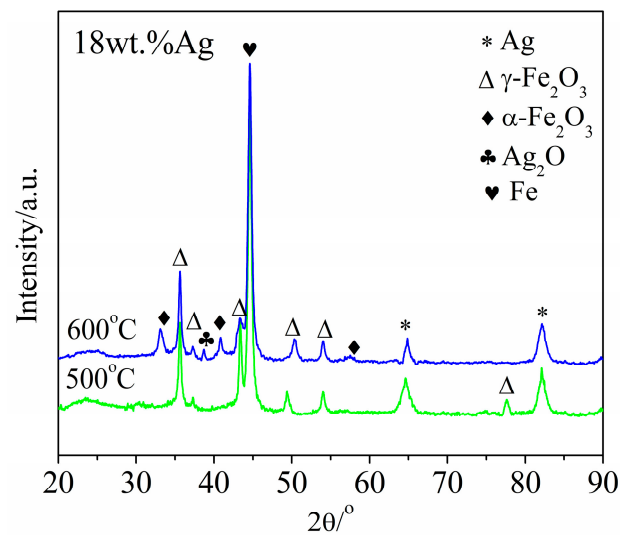**Figure 18.** The worn surface of the nanocomposite coatings with different Ag contents and the ball at 600 °C.

### 3.3. High-Temperature Lubrication Mechanism of the Nanocomposite Coatings

Ag and γ-Fe_2O_3 are beneficial to forming a continuous and dense lubricating film on the worn surface, which significantly improves the wide-temperature tribological properties of the friction pair of the nanocomposite coatings and ball. XRD analysis of the worn surfaces of the nanocomposite coatings is performed to explain the high-temperature lubrication mechanism at 500 °C and 600 °C. Figure 19 shows the XRD results of the worn surface on the nanocomposite coatings under different Ag contents.

(**a**) 10 wt.%Ag

(**b**) 18 wt.%Ag
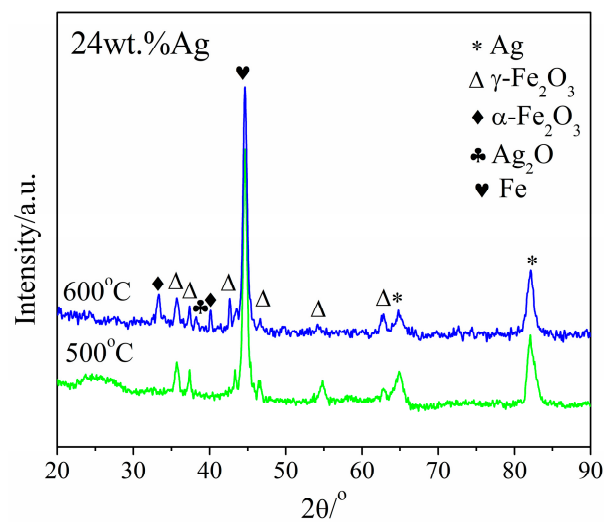
(**c**) 24 wt.%Ag

Figure 19. XRD of the worn surface on the nanocomposite coatings under different Ag contents and temperatures.

It is shown that there is no new phase generated on the worn surface of the nanocomposite coatings at 500 °C. From RT to 300 °C, Ag plays a role in lubricating and reducing the friction of the nanocomposite coatings. At RT, the lubricating films, including Ag, are discontinuous due to the slow diffusion of Ag, resulting in a high CoF. The stable CoF at 100 °C and 300 °C is low compared with that at RT. Ag is diffused rapidly from the nanocomposite coatings to the worn surface, and a more continuous lubricating film can be formed on the worn surface with increases in temperature. At 500 °C, γ-Fe$_2$O$_3$ becomes soft and is sheared easily under the action of the ambient temperature and the friction heat. It formed a continuous lubricating film with Ag, which plays a synergistic role in reducing friction. Therefore, the γ-Fe$_2$O$_3$@SiO$_2$-Ag nanocomposite coatings show good high-temperature tribological properties at 500 °C. At 600 °C, the γ-Fe$_2$O$_3$ was transferred partially into α-Fe$_2$O$_3$ on the worn surface of the nanocomposite coatings. There is a diffraction peak of Ag$_2$O on the worn surface, indicating that Ag is oxidized partially according to the XRD results. These results of α-Fe$_2$O$_3$ and Ag$_2$O result in a high CoF of the nanocomposite coatings.

Ag is distributed in the γ-Fe$_2$O$_3$@SiO$_2$-Ag nanocomposite coatings and plays an important antifriction role from RT to 300 °C. With the increase in temperature, Ag can easily form a continuous lubricating film on the contact surface of the friction pair, resulting in a low CoF. When the temperature rises to 500 °C, γ-Fe$_2$O$_3$ becomes soft and is sheared, reducing the friction and wear of the nanocomposite coatings under the synergism effect of Ag. For the nanocomposite coatings with different Ag contents, it is easy to form a continuous lubricating film with the increase in Ag content at the same temperature, which plays a role in anti-friction lubrication.

In summary, with the increase in Ag content, the curve fluctuation of the CoF at different temperatures decreases and the value of the CoF at the stable stage decreases. Figure 20 shows the diagram of the friction mechanism of the nanocomposite coatings. At 500 °C and 600 °C, the 24 wt.%Agγ-Fe$_2$O$_3$@SiO$_2$-Ag nanocomposite coatings reach a low CoF of 0.06 and 0.05, respectively. Running-in time is about 1500 s and 1100 s, respectively. At all temperatures, the volume wear rate of γ-Fe$_2$O$_3$@SiO$_2$-Ag nanocomposite coatings containing Ag is low compared to γ-Fe$_2$O$_3$@SiO$_2$ nanocomposite coatings without Ag, indicating that γ-Fe$_2$O$_3$@SiO$_2$-Ag nanocomposite coatings have a good anti-wear effect. At RT, with the increase in Ag content, the lamellar films on the wear surface of the nanocomposite coatings decrease gradually. When the temperature rises, due to the increased shear capacity of Ag and γ-Fe$_2$O$_3$ in the nanocomposite coatings, a good anti-friction lubrication film is generated on the wear surface, especially at 500 °C, and the coatings with different Ag contents can reach a CoF of less than 0.1. The 18 wt.%Ag and 24 wt.%Ag nanocomposite coatings have low CoFs of 0.05 and 0.06, respectively. The high-temperature lubrication mechanism of γ-Fe$_2$O$_3$@SiO$_2$ nanocomposite coatings is attributed to the lubrication films of the nanocrystalline γ-Fe$_2$O$_3$ with low shear strength on the friction interface of the nanocomposite coatings, which result in excellent high-temperature self-lubrication performances from the γ-Fe$_2$O$_3$@SiO$_2$ nanocomposite coatings.
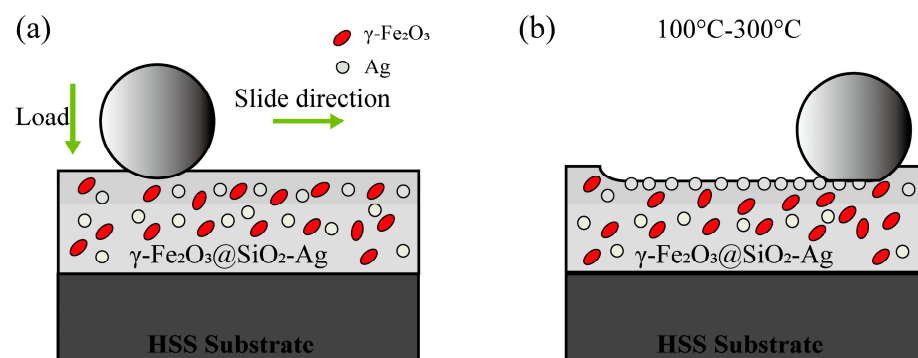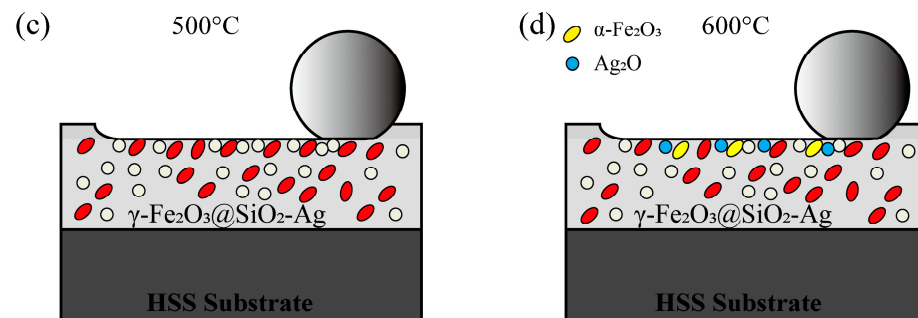

Figure 20. *Cont.*

Figure 20. The diagram of the friction mechanism of the nanocomposite coatings: (**a**) RT, (**b**) 100–300 °C, (**c**) 500 °C, (**d**) 600 °C.

4. Conclusions

The γ-Fe$_2$O$_3$@SiO$_2$-Ag nanocomposite coatings were prepared using the sol-gel method on high-speed steel. The microstructure and wide-temperature tribological properties of the nanocomposite coatings were studied over a wide temperature range from RT to 600 °C. The conclusions are as follows:

(1) The microstructure and mechanical properties of γ-Fe$_2$O$_3$@SiO$_2$-Ag nanocomposite coatings are influenced by the Ag content. There are holes in the nanocomposite coatings at the Ag content of 10 wt.% and 18 wt.%. The microstructure of the nanocomposite coatings is dense at the Ag content of 24 wt.%.

(2) The CoF and wear rate of γ-Fe$_2$O$_3$@SiO$_2$-Ag nanocomposite coatings decrease gradually with the increase in Ag content from RT to 300 °C.

(3) At 500 °C, the lowest CoFs of 10 wt.%Ag, 18 wt.%Ag, and 24 wt.%Ag in the γ-Fe$_2$O$_3$@SiO$_2$ nanocomposite coatings are 0.08, 0.05, and 0.06, respectively. At 600 °C, the CoFs of 10 wt.%Ag, 18 wt.%Ag, and 24 wt.%Ag in the γ-Fe$_2$O$_3$@SiO$_2$ nanocomposite coatings decrease first and then increase, and the wear rate of the Ag-doped nanocomposite coatings is low compared with that of the nanocomposite coatings without Ag.

(4) Ag plays a role in lubricating and reducing wear from RT to 300 °C. At 500 °C, γ-Fe$_2$O$_3$ in the γ-Fe$_2$O$_3$@SiO$_2$ nanocomposite coatings becomes soft due to the friction heat and the environment temperature and is easy to shear and lubricate with Ag. The CoF of the nanocomposite coatings is as low as 0.1. At 600 °C, the tribological properties of the nanocomposite coatings become worse due to the oxidation of Ag and the phase transition of γ-Fe$_2$O$_3$ in the nanocomposite coatings.

Author Contributions: Conceptualization, Q.Z. and Q.J.; methodology, Q.Z. and Q.J.; software, S.S. and Q.J.; validation, Q.Z. and S.S.; formal analysis, Q.Z., Q.J. and S.S.; investigation, Q.Z. and S.S; resources, Q.Z.; data curation, Q.Z. and S.S.; writing—original draft preparation, Q.Z. and S.S.; writing—review and editing, Q. Z., S.S. and Q.J.; visualization, Q.Z. and S.S.; supervision, Q.Z.; project administration, Q.Z.; funding acquisition, Q.Z. All authors have read and agreed to the published version of the manuscript.

Data Availability Statement: The original contributions presented in the study are included in the article, further inquiries can be directed to the corresponding author.

Conflicts of Interest: The authors declare no conflicts of interest.

References

1. Ouyang, J.-H.; Li, Y.-F.; Zhang, Y.-Z.; Wang, Y.-M.; Wang, Y.-J. High-temperature solid lubricants and self-lubricating composites: A critical review. *Lubricants* **2022**, *10*, 177. [CrossRef]
2. Voevodin, A.; Zabinski, J. Nanocomposite and nanostructured tribological materials for space applications. *Compos. Sci. Technol.* **2005**, *65*, 741–748. [CrossRef]
3. Erdemir, A.; Voevodin, A.A. Nanocomposite coatings for severe application. In *Handbook of Deposition Technologies for Films and Coatings*, 3rd ed.; Martin, P.M., Ed.; William Andrew Publishing: Norwich, NY, USA, 2010; pp. 679–715. [CrossRef]
4. Wang, J.Y.; Shan, Y.; Guo, H.; Li, B.; Wang, W.; Jia, J. Friction and wear characteristics of hot-pressed NiCr–Mo/MoO$_3$/Ag self-lubrication composites at elevated temperatures up to 900 °C. *Tribol. Lett.* **2015**, *59*, 48. [CrossRef]
5. Findik, F. Latest progress on tribological properties of industrial materials. *Mater. Des.* **2014**, *57*, 218–244. [CrossRef]
6. Semenov, A. Tribology at high temperatures. *Tribol. Inter.* **1995**, *28*, 45–50. [CrossRef]
7. Kasar, A.K.; Scalaro, K.; Menezes, P.L. Tribological properties of high-entropy alloys under dry conditions for a wide temperature range—A review. *Materials* **2021**, *14*, 5814. [CrossRef] [PubMed]
8. Zhu, S.; Cheng, J.; Qiao, Z.; Yang, J. High temperature solid-lubricating materials: A review. *Tribol. Int.* **2019**, *133*, 206–223. [CrossRef]
9. Zeng, Q.; Qi, W. High temperature superlubricity behaviors achieved by AlSiN coatings against WS$_2$ coatings at 600 °C. *Ceram. Int.* **2024**, *50*, 3787–3796. [CrossRef]
10. Jin, B.; Zhao, J.; Chen, G.; He, Y.; Huang, Y.; Luo, J. In situ synthesis of Mn$_3$O$_4$/graphene nanocomposite and its application as a lubrication additive at high temperatures. *Appl. Surf. Sci.* **2021**, *546*, 149019. [CrossRef]
11. Zeng, Q.; Cai, S. Low-friction behaviors of Ag-doped γ-Fe$_2$O$_3$ @SiO$_2$ nanocomposite coatings under a wide range of temperature conditions. *J. Sol-Gel Sci. Technol.* **2019**, *90*, 271–280. [CrossRef]
12. Xu, X.; Sun, J.; Su, F.; Li, Z.; Chen, Y.; Xu, Z. Microstructure and tribological performance of adaptive MoN–Ag nanocomposite coatings with various Ag contents. *Wear* **2022**, *488*, 204170. [CrossRef]
13. Chen, Y.; Sun, J.; Liu, Y.; Li, Q.; Xiao, S.; Su, F. Microstructure, mechanical and high-temperature tribological properties of MoS$_2$-Cr-Ag composite films. *Surf. Coat. Technol.* **2023**, *452*, 129135. [CrossRef]
14. Yan, Z.; Liu, J.; Shi, X.; Wang, C.; Lu, X.; Hao, J. Tribological properties and transfer behaviors of WS$_2$-Ag nanocomposite films with structure evolution for aerospace application. *Appl. Surf. Sci.* **2024**, *674*, 160928. [CrossRef]
15. Huang, K.; Cao, X.; Kong, L.; Lu, Z.; Zhang, G.; Ding, Q.; Hu, H. Effect of Ag content on friction and wear properties of Ag and V co-doped CrN coatings at 25–700 °C. *Ceram. Int.* **2021**, *47*, 35021–35028. [CrossRef]
16. Patnaik, L.; Maity, S.R.; Kumar, S. Comprehensive structural, nanomechanical and tribological evaluation of silver doped DLC thin film coating with chromium interlayer (Ag-DLC/Cr) for biomedical application. *Ceram. Int.* **2020**, *46*, 22805–22818. [CrossRef]
17. Zeng, Q. Thermal stability and high-temperature super low friction of γ-Fe$_2$O$_3$ @SiO$_2$ nanocomposite coatings on steel. *Lubricants* **2024**, *12*, 223. [CrossRef]
18. Zeng, Q.; Cai, S.; Li, S. High-temperature low-friction behaviors of γ-Fe$_2$O$_3$ @SiO$_2$ nanocomposite coatings obtained through sol–gel method. *J. Sol-Gel Sci. Technol.* **2018**, *85*, 558–566. [CrossRef]
19. Ju, H.; He, S.; Yu, L.; Asempah, I.; Xu, J. The improvement of oxidation resistance, mechanical and tribological properties of W$_2$N films by doping silicon. *Surf. Coat. Technol.* **2017**, *317*, 158–165. [CrossRef]
20. Liu, Y.; Chen, X.; Li, J.; Luo, J. Enhancement of friction performance enabled by a synergetic effect between graphene oxide and molybdenum disulfide. *Carbon* **2019**, *154*, 266–276. [CrossRef]
21. Velasco, S.; Cavaleiro, A.; Carvalho, S. Functional properties of ceramic-Ag nanocomposite coatings produced by magnetron sputtering. *Prog. Mater. Sci.* **2016**, *84*, 158–191. [CrossRef]
22. Fu, Y.; Li, H.; Ji, L.; Liu, X.; He, N.; Zhou, H.; Chen, J. Preparation and high-temperature tribological properties of CrAlVYN-Ag nanocomposite coatings. *Mater. Manuf. Process.* **2017**, *32*, 409–415. [CrossRef]
23. Feng, X.; Lu, C.; Jia, J.; Xue, J.; Wang, Q.; Sun, Y.; Wang, W.; Yi, G. High temperature tribological behaviors and wear mechanisms of NiAl–NbC–Ag composites formed by in-situ decomposition of AgNbO$_3$. *Tribol. Int.* **2020**, *141*, 105898. [CrossRef]
24. Bondarev, A.; Golizadeh, M.; Shvyndina, N.; Shchetinin, I.; Shtansky, D. Microstructure, mechanical, and tribological properties of Ag-free and Ag-doped VCN coatings. *Surf. Coat. Technol.* **2017**, *331*, 77–84. [CrossRef]
25. Vidiš, M.; Truchlý, M.; Izai, V.; Fiantok, T.; Rajninec, M.; Roch, T.; Satrapinskyy, L.; Haršáni, M.; Nagy, Š.; Turiničová, V.; et al. Mechanical and tribological properties of Ag/TiB$_x$ nanocomposite thin films with strong antibacterial effect prepared by magnetron co-sputtering. *Coatings* **2023**, *13*, 989. [CrossRef]
26. Dong, Y.; Wang, Z.; Yuan, J.; Wang, Z.; Zhang, Y.; Ma, G.; Wang, A. Temperature-adaptive lubrication of Ag doped Cr$_2$AlC nanocomposite coatings. *Wear* **2024**, *540*, 205221. [CrossRef]

27. Lozano, D.; Mercado-Solis, R.; Perez ATalamantes, J.; Morales, F.; Hernandez-Rodriguez, M. Tribological behaviour of cast hypereutectic Al–Si–Cu alloy subjected to sliding wear. *Wear* **2009**, *267*, 545–549. [CrossRef]
28. Weibel, A.; Bouchet, R.; Boulc, F.; Knauth, P. The big problem of small particles: A comparison of methods for determination of particle size in nanocrystalline anatase powders. *Chem. Mater.* **2005**, *17*, 2378–2385. [CrossRef]